Nanocrystalline zinc–nickel alloy deposition using pulse electrodeposition (PED) technique

M. Ilayaraja, S. Mohan*, R. M. Gnanamuthu and G. Saravanan

Zinc–nickel alloy was electrodeposited on stainless steel using pulse current deposition (PED) from a chloride–sulphate bath. Duty cycles were varied between 10 and 80% and frequency was changed from 10 to 100 Hz. The deposit characteristics were analysed using SEM, XRD and AFM and the results are presented in this paper. The corrosion resistance of zinc–nickel alloy deposited from direct current deposition (DCD) has been compared with that of the deposit obtained by pulse current using the electrochemical impedance spectroscopy method.

Keywords: Zn–Ni, Pulse electrodeposition, XRD, AFM, Potentiodynamic polarisation

Introduction

Many alternatives are being developed to the well established use of zinc coatings on steel; to improve its corrosion behaviour, zinc–nickel alloy coatings have proved to be very effective because they are far superior to pure zinc deposits for both corrosion resistance and thermal stability. Extensive studies have been carried out on electrodeposition of such alloys from different baths, e.g. chloride–sulphate,[1,2] sulphate and chloride baths.[3,4] Because such zinc alloy deposits provide better corrosion protection than electrogalvanised coating,[5–8] alloys of zinc with metals such as iron, nickel and cobalt have been considered as prime candidates to replace zinc as protective coating. In particular, studies have shown that the corrosion resistance of electrodeposited Zn–Ni alloy coatings, within a certain composition range (12–15%) of Ni, can be five to six times better than for pure zinc of equal thickness[9–11] by pulse electrodeposition (PED), which, compared with DCD, can improve the deposition process and some deposit properties in addition to corrosion resistance, namely, porosity, ductility, hardness and surface roughness.[12–14]

In the present work, the authors have studied zinc–nickel alloy deposits by PED on stainless steel, with a pre-alloy plating nickel strike: it is difficult to do electroplate on stainless steel because of the presence of its passive layer. This passive layer is removed by a suitable pretreatment in acid solution. In this paper, composition, morphology, hardness and corrosion resistance using SEM, AFM, XRD and EIS were investigated.

The square-wave cathodic pulse is presently the most widely used method of modulating plating current. In direct current deposition (DCD), only one current- and time-dependent variable, namely, the current density, can be controlled, whereas in PED, three parameters are independently variable, pulse peak current, pulse on time and pulse off time, which determine the physical characteristics of the deposits obtained from a given electrolyte. Pulse electrodeposition improves the current distribution altering the prevailing mass transport conditions[15,16] controlling the microstructure, increasing brightness and decreasing porosity, internal stress and impurities.[17–19]

Central Electrochemical Research Institute, Karaikudi 630 006, India

*Corresponding author, email sanjnamohan@yahoo.com

Experimental

Surface preparation of substrates

An electrolyte consisting of 325 g L^{-1} $ZnSO_4$, 200 g L^{-1} $NiCl_2$, 40 mL L^{-1} glacial acetic acid and 0·1 g L^{-1} sodium lauryl sulphate were prepared using doubly distilled water and AnalaR grade chemicals. Electrodeposition of zinc–nickel alloy on stainless steel cathodes was carried out after a nickel strike in a solution consisting of nickel chloride (1·009M) and concentrated hydrochloric acid (20%). Graphite was employed as the anode for zinc–nickel alloy deposition. The procedure for alloy plating consisted of the following sequence of operations.

The polished substrates were degreased with acetone and then cathodically cleaned in alkaline solution containing sodium hydroxide (35 g L^{-1}) and sodium carbonate (25 g L^{-1}) for 2 min at 70°C, and rinsed with distilled water. Acid etching was carried out with 20%HCl. Pulse plating of Zn–Ni layers was then carried out on the smooth and clean stainless steel panels. Measurements of pH were made using Testronics 511 digital pH meter. The pH of the bath was maintained at 3·5–4, using 5%H_2SO_4. The pulse plating parameters used in the PED technique are given in Table 1.[20]

Pulse plating of Zn–Ni

Pulse plating was carried out using a Dynatronix model DPR 20-5-10 supply unit.

The formulae used for determining various parameters are given below

$$\text{Duty cycle} = \frac{\text{on time}}{\text{on time} + \text{off time}} \times 100\%$$

Published by Maney on behalf of the Institute
Received 3 September 2007; accepted 16 January 2009
DOI 10.1179/174591909X438947

$$\text{Average current} = \frac{\text{on time} \times \text{peak current}}{\text{total time}}$$

$$\text{Peak current} = \frac{\text{average current}}{\text{duty cycle}}$$

Deposit characterisation

Crystallographic structures of the Zn–Ni alloy coatings were analysed with an X'Pert Pro Philips X-ray diffractometer using Cu K_α line. The microstructure of the coatings was examined using a Hitachi S 3000H scanning electron microscope and a molecular imaging atomic force microscope. The microhardness of the Zn–Ni coated steels was evaluated using DM 400 microhardness tester from LECO with Vickers indentors. A diamond pyramid was pressed into the deposit under a load of 25 g for 15 s and the indentation diagonal measured after the load was removed. The microhardness in kg mm^{-2} was determined in each case using the formula

$$H_V = 1854\frac{L}{d^2}$$

where L is the applied load in g and d is the diagonal of the indentation in μm.

The surface morphology of the zinc–nickel deposit formed by PED was studied by a Hitachi 3000H SEM. Surface topography examinations were carried out by molecular imaging atomic force microscopy.

Corrosion resistance studies

The corrosion resistance of Zn–Ni alloy deposited by DCD and PED was assessed by potentiodynamic polarisation and electrochemical impedance spectroscopy studies.

Potentiodynamic polarisation and electrochemical impedance studies

The electrochemical studies were carried out with the advanced electrochemical system Parstat 2273. Electrochemical impedance spectroscopy measurements on the PED zinc–nickel alloys were carried out in the same three electrode assembly as used for the potentiodynamic polarisation experiments. Impedance were recorded at open circuit potential (OCP) applying an ac signal in the frequency range from 10 mHz to 100 KHz. The Tafel calculation gives access to the corrosion current regularly present at the surface of a metal which is in contact with a corroding solution. The corrosion is expressed in loss of metal thickness per year. The Tafel method, which is a complete tool to study the corrosion process at a metal surface, also gives access to other corrosion parameters such as the zero current potential (corrosion potential), the corrosion current and the polarisation resistance of the sample under study. Parameters measured include:

(i) the zero current potential E (i=0) as the corrosion current
(ii) the polarisation resistance R_p (a parabolic regression is performed on the curve around the zero current potential, R_p is determined as the slope of the tangent to this parabola at the zero current potential)
(iii) the corrosion current i_{corr}
(iv) the slope b_a of the tangent to the anodic branch of the curve
(v) the slope b_c of the tangent to the cathodic branch of the curve
(vi) the corrosion rate is calculated as iron thickness corroded per year (the atomic mass, valence, density and working electrode area are used to calculate the corrosion rate).

The corrosion rate (CR) is expressed in mils per year, readily converted to microns per year (Table 2)

$$CR = 0{\cdot}1288 i_{corr}\frac{w}{\rho}$$

where i_{corr} is the corrosion current in A cm^{-2}, w is the eqivalent weight of metal and ρ is the density.

The corrosion rate observed on alloy plated samples at 80% duty cycle was significantly lower than that of direct current deposited Zn–Ni alloy on stainless steel.

Results

Influence of thickness of deposit at various frequencies

Figure 1 shows that thickness of deposit increases with increasing pulse duty cycle. The same results are obtained at 5 A dm^{-2}. As the duty cycle increases, current on time increases and off time decreases. At a lower duty cycle, the peak current is flowing for less time and the overall amount of deposition is less when compared with higher duty cycle. Hence, the thickness increases with increasing duty cycle.

Influence of current efficiency

Figure 2 shows that current efficiency increases with increasing pulse frequency. As pulse frequency increases, the pulses are very short and they produce thin diffusion layers. Thus, transport and diffusion of metal ions from bulk electrolyte to the cathode surface through these layers is possible and much easier than through the thick diffusion layers that are obtained at low frequency or with larger pulses. So this enhancement of migration of ions increases the nucleation rate, uniformity and

Table 1 Pulse plating parameters used in PED

	Pulse on–off time, ms				Current density, A dm^{-2}					
	Pulse frequency, Hz									
Duty cycle, %	10	20	50	100	Peak			Average		
10	10–90	4–36	2–18	1–9	40	80	120	4	8	12
20	20–80	8–32	4–36	2–8	20	40	60	4	8	12
40	40–60	16–24	8–12	4–6	10	20	30	4	8	12
80	80–20	32–8	16–4	8–2	5	10	15	4	8	12

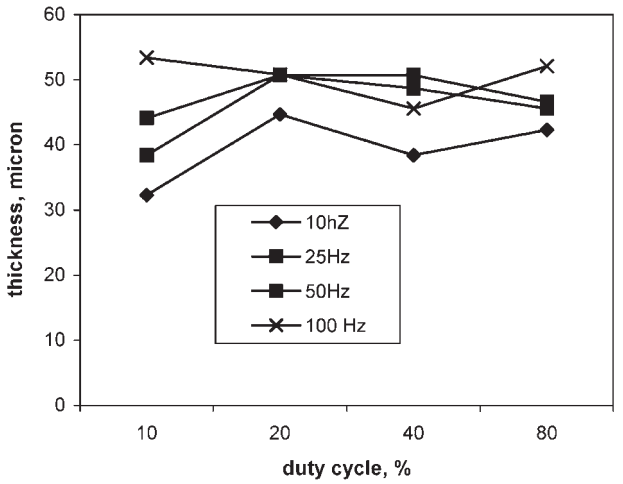

1 Effect of pulse duty cycle on thickness of deposit from Zn–Ni chloride–sulphate bath at various frequencies

deposition rate, and also increases the current efficiency from the chloride–sulphate bath. The same trend is seen when the current is increased at 5 A dm^{-2}.

Microstructure analysis

X-ray diffraction results

The XRD patterns of electrodeposited zinc–nickel alloy from the chloride–sulphate bath at average current density 4 A dm^{-2} are shown in Fig. 3. The electrodeposit consist of strong $NiZn_3$ (13 1 3) plane at 2θ=42·5066°. The crystallite size was calculated using the Debye–Scherrer formula

$$D = \frac{0{\cdot}9\lambda}{\beta \cos\theta}$$

where D is the crystallite size, β is the broadening of diffraction line measured at half of its maximum intensity in radians and λ is the X-ray wavelength (1·5406 Å) used. The calculated crystallite size of $NiZn_3$ (13 1 3) is 59·7 nm, which is attributed to preferred orientation along the (13 1 3) plane. X-ray diffraction results are shown in Table 2.

Scanning electron microscope study

The surface morphologies of the zinc–nickel deposits formed by PED and DCD, studied by the Hitachi 3000H SEM, are given in Figs. 4 and 5 respectively.

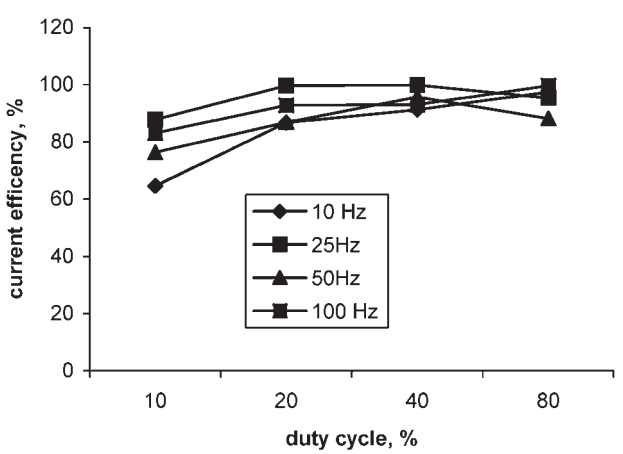

2 Effect of pulse duty cycle on current efficiency of Zn–Ni chloride–sulphate bath at various frequencies

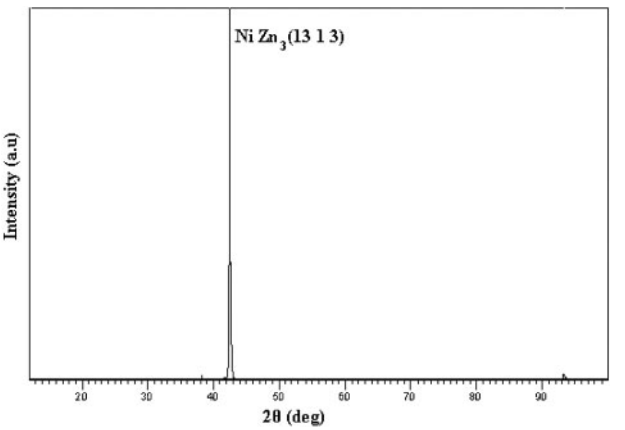

3 X-ray diffraction result from Zn–Ni deposit from chloride–sulphate bath at 5 A dm^{-2}

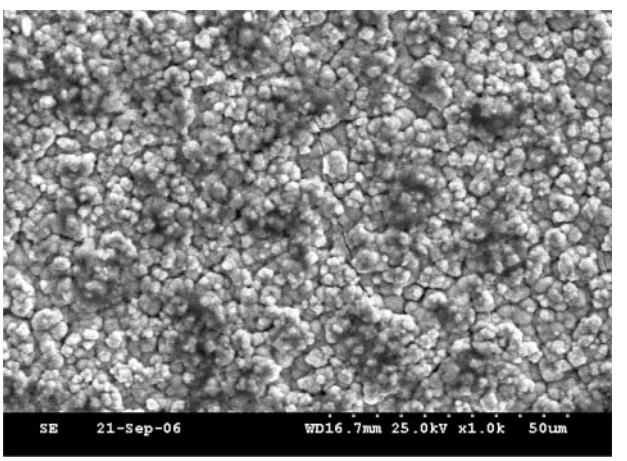

4 Micrograph (SEM) of Zn–Ni deposits from chloride–sulphate bath obtained at DC deposition at 5 A dm^{-2}

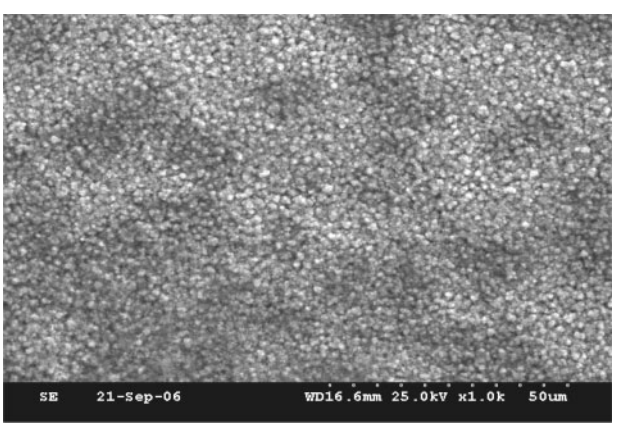

5 Micrograph (SEM) of zinc–nickel alloy deposit obtained at 10% duty cycle

DCD and PED Zn–Ni are obtained at 5 A dm^{-2} and 10% duty cycle. From the SEM figures, PED Zn–Ni has a 0·5–1 μm grain size, whereas a 1–2·5 μm grain size is

Table 2 X-ray diffraction data of Zn–Ni deposit resulting from chloride–sulphate bath at 5 A dm^{-2}

hkl	2θ, °	*d*-spacing	Grain size, nm
$NiZn_3$ (13 1 3)	42·5066	2·12501	59·70

Table 3 Corrosion parameters obtained from impedance studies in 5%NaCl solution

Pulse duty cycle	E_{corr}(SCE), mV	b_a, mV	b_c, mV	I_{corr}, A cm^{-2}	Corrosion rate	
					m py	μm py
PED (80–10%)	−1143·979	94·911	−116·960	$5{\cdot}06\times10^{-5}$	2·971	74
DCD	−983·856	84·549	−170·570	$4{\cdot}580\times10^{-5}$	9·876	247

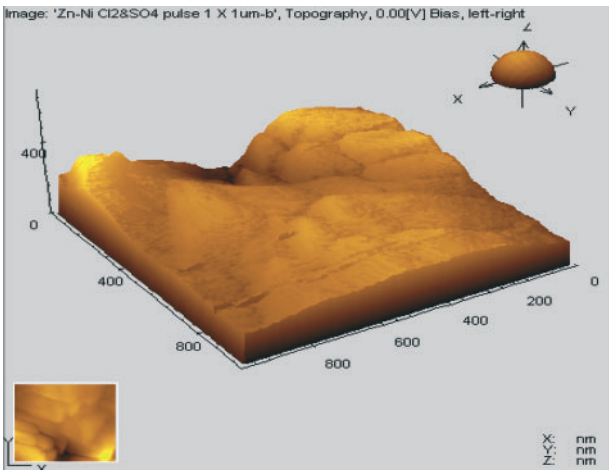

6 Atomic force microscopy images (scan size: 1 × 1 μm) showing topography of PED plating of Zn–Ni alloy on stainless steel

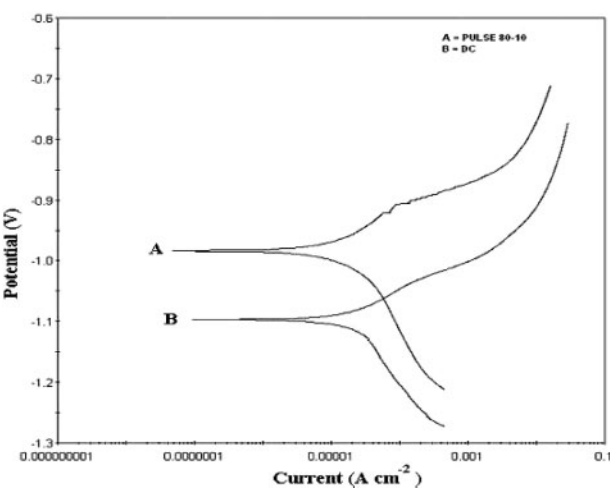

7 Polarisation studies of Zn–Ni alloy on stainless steel in 5% NaCl

obtained in DCD deposits. Since fine grained, nodular and crack free deposits are obtained in PED, it has very good corrosion resistance, superior to that of DCD Zn–Ni.

Atomic force microscopy results

Surface topography examination carried out by molecular imaging atomic force microscopy shows the AFM picture scanned over an area of 1 × 1 μm of the zinc–nickel alloy plated on stainless steel prepared under the optimised conditions (Fig. 6). By comparing the SEM and AFM figures, it seems clear that the structural characteristic of PED Zn–Ni deposit is that it consists of many small spherical particles of ∼500 nm in size.

Corrosion resistance: electrochemical impedance and polarisation resistance

The impedance results obtained from Nyquist plots, and accompanying corrosion behaviour, for the samples used for corrosion tests in 5%NacCl solution, are shown in Table 3, where it can be seen that corrosion rate of the pulse current deposited Zn–Ni alloy sample is less than the direct current deposited sample. This result is supported by the polarisation curve data shown in Table 3 and Fig. 7.

Conclusion

Pulse electroplating of zinc–nickel alloy on stainless steel was carried out from a chloride–sulphate bath at various pulse duty cycles, frequencies and current densities. The pulse plating conditions such as on time, off time, duty cycle and frequency were optimised. From these studies, it may be concluded that smooth and fine grained zinc–nickel alloy deposits can be obtained at 80% duty cycle and frequency 100 Hz. Zn–Ni alloy deposited at 80% duty cycle has the best corrosion resistance, and this is superior to that of direct current deposited Zn–Ni alloy. Using pulse current, improved properties of the deposit were obtained.

References

1. R. G. Baskar and C. A. Holden: *Plat. Surf. Finish.*, 1985, **72**, 54.
2. K. Raeissi, M. A. Golozar, A. Saatchi and J. A. Szpunar: *Trans. IMF*, 2005, **83**, (2), 99–103.
3. R. Alballet, E. Gomez, C. Mulkler, M. Sarret, E. Valles and J. Pregonas: *J. Appl. Electrochem.*, 1990, **20**, 635.
4. E. Chamaing and R. Wairt: *Electrochim. Acta*, 1992, **37**, 545.
5. S. Shanmugasigamani and M. Pushpavanam: *Trans. IMF*, 2008, **86**, (2), 122–128.
6. L. Q. Zhu, F. W. Wang and T. Watanabe: *Trans. IMF*, 2005, **83**, (5), 258.
7. T. J. Tuaweri and G. D. Wilcox: *Trans. IMF*, 2007, **85**, (5), 245.
8. D. E. O. S. Carpenter and J. P. G. Farr: *Trans. IMF*, 2007, **85**, (6), 298.
9. Y. F. Jiang, X. W. Guo, C. Q. Zwari, Y. P. Zho and W. J. Ding: *Trans. IMF*, 2003, **81**, 182–185.
10. S. Franz, A. Marlot, P. L. Cavallotti and D. Landolt: *Trans. IMF*, 2008, **86**, 92–97.
11. J. M. Yang, D. Zhu and D. H. Kim: *Trans. IMF*, 2008, **86**, (2), 98–102.
12. J. C. Puippe and F. H Leaman (eds.): 'Theory and practice of pulse plating'; 1986, Orlando, FL, AESF Society.
13. R. Alballet, E. Gomez, C. Mulkler, M. Sarret, E. Valles and J. Pregonas: *J. Appl. Electrochem.*, 1991, **21**, 44.
14. R. Ramanauskies and R. Juskeres Liet: *Moksimi Aked Chem.*, 1991, **3**, 57.
15. N. Masuko, T. Osaka and Y. Ito (eds.): 'New trends and approaches in electrochemical technology'; 1996, New York, John Wiley & Sons.
16. S. I. Kwak, K. M. Jeong, S. J. Kim and H. J. Sohn: *J. Electrochem. Soc.*, 1996, **143**, 2770.
17. M. Datta and D. Landolt: *Surf. Technol.*, 1985, **25**, 97.
18. M. Halmdienst, W. E. G. Hansal, G. Kaltenhauser and W. Kautek: *Trans. IMF*, 2007, **85**, (1), 22.
19. C. Suarez, E. Chavez, J. A. Diez, H. Grande and R. Guixa: *Trans. IMF*, 2007, **85**, (1), 46.
20. G. Devaraj and S. K. Seshadri: *Plat. Surf. Finish.*, 1996, **83**, (6), 62–66.